GOLD(I) COMPLEX OF 1,1'-BIS(DIPHENYLPHOSPHINO)FERROCENE-QUINOLINE CONJUGATE: A VIROSTATIC AGENT AGAINST HIV-1

Ntombenhle Gama,[a] Kamlesh Kumar,[b,c] Erik Ekengard,[b] Matti Haukka,[d] James Darkwa,[c] Ebbe Nordlander,[b] and Debra Meyer,[a,e]

[a]*Department of Biochemistry, University of Pretoria, Hatfield Campus, Pretoria 0002, South Africa*

[b]*Inorganic Chemistry Research Group, Chemical Physics, Center for Chemistry and Chemical Engineering, Lund University, Box 124, SE-22100 Lund, Sweden.*

[c]*Department of Chemistry, University of Johannesburg, Kingsway campus, Auckland Park, South Africa, 2006.*

[d]*Department of Chemistry, University of Jyväskylä, FI-40014, Finland.*

[e]*Dean's Office, Faculty of Science, University of Johannesburg, Kingsway Campus, Johannesburg , Auckland Park 2006, South Africa (Current address)*

Corresponding authors: D.Meyer (dmeyer@uj.ac.za)
J. Darkwa (jdarkwa@uj.ac.za)
E. Nordlander (ebbe.nordlander@chemphys.lu.se)

ABSTRACT

HIV infection is known for replication in proliferating CD^+ T-cells. Treatment of these cells with cytostatic (anti-proliferation) compounds such as hydroxyurea interferes with the cells's ability support HIV replication. Combinations of such cytostatic compounds with proven anti-retroviral drugs (like ddI) are known as virostatic , and have been shown to aid in the control of the infection. The use of two different drugs in virostatic combinations however, carries the risk of adverse effects including drug-drug interactions, which could lead to augmented toxicities and reduced efficacy. Here, a novel digold(I) complex of ferrocene-quinoline (**3**) was investigated for cytostatic behaviour as well as anti-viral activity which if demonstrated would eliminate concerns of drug-drug interactions. The complex was synthesized and characterized by NMR, FT-IR and mass spectroscopy and the molecular structure was confirmed by X-ray crystallography. Bio-screening involved viability dyes, real time electronic sensing and whole virus assays. The complex showed significant (p = 0.0092) inhibition of virus infectivity (83%) at 10 ug/mL. This same concentration caused cytostatic behaviour in TZM-bl cells with significant (p<0.01) S and G2/M phase cell cycle arrest. These data supports **3** as a virostatic agent, possessing both anti-viral and cytostatic characteristics.

INTRODUCTION

Human Immunodeficiency Virus (HIV), the etiological agent of the Acquired Immune Deficiency Syndrome (AIDS) was responsible for close to 1.2 million deaths in 2014 (World Health Organization 2015). The virus primarily attacks CD4 T-lymphocytes of the immune system resulting in the depletion of these cells (Brenchley et al. 2004). Because HIV can only replicate in proliferating cells, there has been investigations into the use of cytostatic agents (compounds that arrest cell proliferation without actually killing the cells) in combination with known antiviral agents (for direct interaction with the virus while the cells' growth is halted) (Lori et al. 2005; d'Ettorre et al. 2011). The most commonly known virostatic combination is the hydroxyurea-didanosine regimen which has been shown to limit immune activation and suppress viral load (Lori et al. 1999; García et al. 2003). Although the combination of a cytostatic and anti-viral drug may be effective, drug combinations are often associated with adverse drug-drug interactions which may result in toxicity. The development of a single compound exhibiting both anti-viral and cytostatic behaviour would therefore be of benefit in the elimination of possible drug-drug interactions (Pollack et al. 2009).

Apart from drug-drug interactions, another major issue with current drugs used in virostatic combinations are adverse effects which include AZT-associated anaemia and retinoid toxicity, mainly related to protease inhibitors (Montessori et al. 2004). One of the most recently proposed strategies in drug discovery for the elimination of toxicity is the repurposing of already existing drugs with known pharmacological properties, through processes such as lead diversification (Muthyala 2011). Lead diversification is defined as the functionalization of compounds to generate novel analogues which can offer benefits such as tuning of physiochemical properties as well as the removal of toxicophores (Abid Masood et al. 2012). One such drug that has shown great success is the anti-malarial chloroquine. Chloroquine has over the years been one of the most widely used drugs against various species of the malaria parasite, however, the emergence of resistant parasite strains has resulted in its investigation on other pathogens (Krogstad et al. 1987).

Previous reports on metal based modifications of chloroquine such as the addition of gold led to the drug $[Au(CQ)(PPh_3)][PF_6]$, exhibiting 9 times the activity of chloroquine against chloroquine-resistant *P.falciparum* strains and 22 times more activity against rodent malaria (Sánchez-Delgado and Anzellotti 2004). Unmodified chloroquine has also been reported to possess anti-HIV activity against whole viruses (Savarino et al. 2001). Knowing if this activity would improve if chloroquine had gold atoms attached was investigated here. A

digold(I) complex (**3**) derived from 1,1'-bis(diphenylphosphino)ferrocene-quinoline conjugate system (**2**) was examined for its viral inhibitory and anti-proliferative activities to allow comment on its use as a possible virostatic agent.

MATERIALS AND METHODS

All synthetic procedures for compounds **2** and **3** were performed under dry nitrogen using standard Schlenk and vacuum-line techniques. Solvents used for the reactions were dried by distillation over appropriate drying reagents and stored over molecular sieves under nitrogen. All chemicals used in the synthesis were purchased from Sigma-Aldrich and used as received. NMR spectra were recorded on a Varian Inova 500 MHz spectrometer using the solvent resonance as internal standard for ^{1}H NMR and ^{13}C NMR shifts. Chemical shifts in ^{31}P NMR spectra are reported in parts per million (ppm) relative to H_3PO_4 at 0.000 ppm. Infrared spectra were recorded on a Nicolet Avatar 360 FT-IR spectrometer. Electrospray ionization (ESI) mass spectra were recorded using a Waters Micromass Q-Tof micro mass spectrometer.

Synthesis of 1,1'-bis(diphenylphosphino)ferrocene-quinoline conjugate (2)

N,N′-Dicyclohexylcarbodiimid (0.110 g, 0.53 mmol) was added to the solution of **1** (0.370 g, 0.53 mmol) and 2,3,4,5,6-pentafluorophenol (0.127 g, 0.69 mmol) in dry dichlorormethane (35 mL) under nitrogen atmosphere. After stirring the reaction mixture at room temperature for 5 h, N1-(7-chloroquinolin-4-yl)ethane-1,2-diamine (0.155 g, 0.69 mmmol) and diisopropylethyl amine (185 μL) were added. The reaction mixture was stirred further for 20 h under nitrogen atmosphere. The solvent was removed under reduced pressure and crude product was purified by column chromatography using dichloromethane and methanol solvent mixture (92:8 v/v) as eluent. Yield: 0.355 g (~74 %). ^{1}H NMR (500 MHz, $CDCl_3$, δ ppm): 8.44 (d, 1H, J = 5.8 Hz), 8.04 (s, 1H), 8.00 (d, 1H, J = 8.8 Hz), 7.51 (bs, 1H), 7.45 (d, 1H, J = 8.6 Hz), 7.38-7.19 (m, 18H), 7.09-7.06 (m, 2H), 6.28 (d, 1H, J = 5.8 Hz), 5.40 (d, 1H, J = 7.5 Hz, $CH_3CHN\underline{H}CO$), 5.15-5.12 (m, 1H, $CH_3C\underline{H}NH$), 4.38 (s, 2H, Fc), 4.12 (d, 2H, J = 7.3 Hz, Fc), 4.06 (s, 1H, Fc), 3.71-3.64 (m, 1H), 3.58 (d, 2H, J = 9.0 Hz, Fc), 3.56-3.50 (m, 1H), 3.46-3.35 (m, 2H), 2.17-2.13 (m, 2H), 2.00-1.94 (m, 1H), 1.41-1.35 (m, 1H), 1.26 (d, 3H, J = 6.7 Hz $CHC\underline{H_3}$). ^{13}C NMR (125 MHz, $CDCl_3$, δ ppm): 175.25, 170.12, 151.27, 150.02, 147.02, 139.71 (d, J_{P-C} = 10.0 Hz), 138.92 (d, J_{P-C} = 10.0 Hz), 138.07 (d, J_{P-C} = 8.7 Hz), 135.95 (d, J_{P-C} = 7.5 Hz), 135.75, 134.88 (d, J_{P-C} = 21.2 Hz), 133.62 (d, J_{P-C} = 20.0 Hz), 133.02 (d, J_{P-C} = 18.7 Hz), 132.20 (d, J_{P-C} = 18.7 Hz), 129.42, 128.73, 128.44, 128.34, 128.29,

128.25, 128.24, 128.21, 128.19, 128.16, 128.15, 128.09, 126.64, 125.76, 122.81, 117.03, 97.94, 94.56(d, J_{P-C} = 23.7 Hz), 75.65, 75.56, 75.40, 75.25, 74.25 (dd, J_{P-C} = 5 Hz, 1.2 Hz), 73.32, 73.24, 73.13, 73.03, 73.00, 71.59 (dd, J_{P-C} = 5 Hz, 1.2 Hz), 71.41 (d, J_{P-C} = 2.5 Hz), 45.08, 44.54 (d, J_{P-C} = 7.5 Hz), 38.57, 31.64, 30.74, 20.29. ^{31}P NMR ($CDCl_3$, δ ppm): -18.00 (s), -25.69 (s). IR (KBr) ν_{max}/cm^{-1}: 3288w, 3050m, 2925m, 1648w, 1611m, 1581s, 1540m, 1496m, 1432m. (ESI, m/z): 901 $[M+H]^+$.

Synthesis of digold(I) complex (3)

A solution of compound **2** (0.030 g, 0.033 mmol) in dry dichloromethane (5 mL) was added to the solution of [Au(tht)Cl] (0.020 g, 0.066 mmol) in dry dichloromethane (7 mL). The reaction mixture was stirred at room temperature for 40 min under N_2 atmosphere. After reducing solvent volume (3 mL) on rotary evaporator, reaction mixture was poured into the ether (15 mL) yielding light yellow precipitate of titled complex. The precipitate was filtered, dried and further purified by column chromatography using dichloromethane and methanol solvent mixture (90:10) as eluent. Yield: 0.040 g (~ 88%). ^{1}H NMR (500 MHz, $CDCl_3$, δ ppm): 8.40 (d, 1H, J = 10.0 Hz), 8.11-8.09 (m, 2H), 7.73 (bs, 1H), 7.63-7.29 (m, 21H), 6.42 (d, 1H, J = 5.0 Hz), 5.54-5.49 (m, 1H, $CH_3C\underline{H}NH$), 5.13 (bs, 1H, $CH_3CHN\underline{H}CO$), 4.99 (s, 1H, Fc), 4.74 (s, 1H, Fc), 4.69 (s, 1H, Fc), 4.64 (s, 1H, Fc), 4.46 (s, 1H, Fc), 4.12(s, 1H, Fc), 3.81-376 (m, 2H), 3.64-3.57 (m, 2H), 3.52-3.48 (m, 1H), 2.22-2.07 (m, 3H), 1.89-1.83 (m, 2H), 1.08 (d, 3H, J = 6.4 Hz $CHC\underline{H_3}$). ^{13}C NMR (125 MHz, $CDCl_3$, δ ppm): 174.68, 170.11, 134.71 (d, J_{P-C} = 13.7 Hz), 133.77 (d, J_{P-C} = 13.7 Hz), 133.13 (d, J_{P-C} = 13.7 Hz), 132.85 (d, J_{P-C} = 13.7 Hz), 132.62, 132.31 (d, J_{P-C} = 3.7 Hz), 132.01 (d, J_{P-C} = 2.5 Hz), 131.93 (d, J_{P-C} = 3.7 Hz), 130.80, 130.30, 130.22, 129.71, 129.63, 129.40 (d, J_{P-C} = 3.7 Hz), 129.28 (t, J_{P-C} = 3.7 Hz), 129.14 (d, J_{P-C} = 5.0 Hz), 129.03, 128.38, 127.86, 125.84, 123.48, 98.31, 94.53 (d, J_{P-C} = 15.0 Hz), 76.18 (d, J_{P-C} = 8.7 Hz), 75.86 (d, J_{P-C} = 12.5 Hz), 75.69, 74.81, 74.77, 74.70, 73.68 (d, J_{P-C} = 8.7 Hz), 44.90, 44.00, 38.50, 31.52, 30.47, 19.68. ^{31}P NMR ($CDCl_3$, δ ppm): 27.29 (s), 22.18 (s). IR (KBr) ν_{max}/cm^{-1}: 3336w, 3054w, 1654m, 1612m, 1581s, 1541w, 1436s, 1171m, 1101s. MS (ESI, m/z): 1329 $[M-Cl]^+$.

X-ray structure determinations

The single crystals suitable for X-ray study were obtained from slow diffusion of hexane into the dichloromethane solution of complex **3**. The crystal of **3** was immersed in cryo-oil, mounted in a Nylon loop and the X-ray diffraction data were collected on a Agilent Supernova diffractometer using Mo Kα radiation (λ = 0.71073 Å) at a temperature of 170(2)

K. For data collection and data reduction, the CrysAlisPro program was used (Agilent Technologies inc., 2013, Yarnton, Oxfordshire, England). The structure was solved by SUPERFLIP (Palatinus and Chapuis 2007) and the refined by full-matrix least-squares methods on F^2. Empirical absorption correction using spherical harmonics, implemented in CrysAlisPro program package was applied to the data. Structural refinement was carried out using SHELXL-2014 (Sheldrick 2008). The crystal under investigation was diffracting only weakly. The C-C distances in the aromatic ring C46-C51 were restrained to be similar. Carbon atoms C37, C38, C44, and C45 were restrained so that their U_{ij} components approximate to isotropic behavior. Also, the anisotropic displacement parameters for C38 and C39 as well as N4, C43, C44, and C45 were constrained to be similar. The solvent of crystallization could not be unambiguously resolved and therefore the contribution of the solvent to the calculated structure factors was taken into account by using the SQUEEZE routine of PLATON (Spek 2009).

HIV-1 Whole Virus Inhibition

Complex **3** was screened for its ability to inhibit the infection of TZM-bl cells by a pseudotyped HIV-1 subtype C virus, ZM53. TZM-bl cells are HeLa cell line derivatives expressing high levels of CD4 and CCR5 as well as endogenously expressed CXCR4 (obtained through the NIH AIDS Reagent Program, Division of AIDS, NIAID, NIH: TZM-bl from Dr. John C. Kappes, Dr. Xiaoyun Wu and Tranzyme Inc.) (Platt et al. 1998; Derdeyn et al. 2000; Wei et al. 2002; Takeuchi et al. 2008; Platt et al. 2009). The assay was performed as described by Mufhandu et al. (2012) (Mufhandu et al. 2012) with slight modifications. The complex was tested at four concentrations (2.5-20 µg/mL). The complex was diluted in DMEM media supplemented with 5% FBS and 60 µl was added to a black 96-well plate. Diluted virus (1:1 dilution, 25 µL) was added to each well and the plate was incubated for 45 minutes at room temperature to allow interaction of the complex with the virus. TZM-bl cells were cultured to confluence in DMEM media supplemented with 5% Hepes Buffer, 1% Gentamicin and 10% FBS; forming complete media. Post trypsinization, the cells were re-suspended in DMEM media containing 5% FBS and DEA-Dextran to a final concentration of 20 µg/mL. The cells were added to the plate containing complex and virus (10 000 cells/well, 50µL) and the plate was incubated for 48 hours (37 °C, 5% CO_2, 90% humidity). The supernatant was then removed (85 µL) and BrightGlo™ Luciferase Assay Substrate (Promega, USA) was added at 50 µL/well. The plate was incubated for 2 minutes in order to

allow for cell lysis, and luminescence was read using the GloMax® Multidetection System (Promega, USA).The percentage virus neutralization was calculated using the formula:

$$\%\text{Neutralization} = \{100-[(RLU_{Complex}-RLU_{Cells})/(RLU_{virus}-RLU_{Cells})] \times 100\}$$

Cell viability Assay

Complex **3** was investigated for its effect on the viability of TZM-bl cells. Briefly, TZM-bl cells were cultured until confluence in DMEM media (Sigma Aldrich, USA) with 3.7g/L $NaHCO_2$, 0.05% (v/v) Gentamycin, 1% (v/v) Antibiotic/Antimitotic and 10% (v/v) Foetal Bovine Serum (growth media) and were plated in 96-well plate (1.0×10^5 cells/mL, incubated overnight). The cells were then treated with various concentrations of the complex **3** ranging from 1.56-100 µg/mL and incubated for 3 days. Thereafter, MTT working solution (5.0 mg/mL MTT in DMEM, 1:5 ratios, Sigma Aldrich, Germany) was added to each well (100 µL) and the plate was incubated for 2 h. Produced formazan crystals were solubilized with acidified isopropanol (1 mL of 1 M HCl: 9 mL propanol) and the absorbance was measured at 550 nm using a microtiter plate reader (Multiskan Ascent, Thermo Labsystems, USA).0

Real-time Electronic Sensing

A real time cell electronic sensing (RT-CES) device (xCELLigence, Roche, Germany), which monitors the effects of compounds on the viability/proliferation of adherent cells in real time (Atienzar et al. 2011; Fonteh et al. 2011) was used to confirm the MTT-determined CC_{50} information for the compound. The assay was performed as previously described by Fonteh et al. (2011) (Fonteh et al. 2011), with slight modifications. Briefly, a pre-titrated cell concentration of 20 000 cells/well were plated into e-plates and allowed to attach for ~24hours at which point the cell index (CI) was 1±0.5 (37° C, 5% CO_2, 95% humidity). Four different concentrations of compound **3** (25, 50, 100 and 200 µM) were tested, and the cells were monitored for three days. Changes in the cell index values indicating cell responses were used to calculate the area under each curve utilizing GraphPad Prism, and a decision tree by Kursterman et al. (2013) (Kustermann et al. 2013) was used to determine whether the compound had significant toxicity or not (**Fig.S1**).

Cell cycle arrest analyses

In the investigation of potential cytostasis, complex **3** was examined for its influence on the cell cycle of TZM-bl cells. The cells were cultured and treated with the complex (10

µg/mL) as described above. Post incubation of 48 h, the BD Cell Cycletest™ Plus DNA Reagent Kit (BD, USA) was used following the manufacturer's instructions. The cells were also treated with a known cytostatic compound, Roscovitine (6 µg/mL) and these data was compared to **3** (Wang et al. 2000).

RESULTS AND DISCUSSION

Synthesis and Characterization

1,1'-Bis(diphenylphosphino)ferrocene-quinoline conjugate (**2**) was successfully synthesized by the amide coupling of a carboxylic acid derivative of 1,1'-bis(diphenylphosphino)ferrocene (**1**)(Bjelosevic et al. 2006) with N1-(7-chloroquinolin-4-yl)ethane-1,2-diamine(Yearick et al. 2008) (**Scheme 1**). The reaction of compound **2** with chloro(tetrahydrothiophene)gold(I), [Au(tht)Cl] in 1:2 molar ratio in dichloromethane at room temperature gave the corresponding gold complex (**3)** in 88% yield (**Scheme 2**) (Uson et al. 1989).

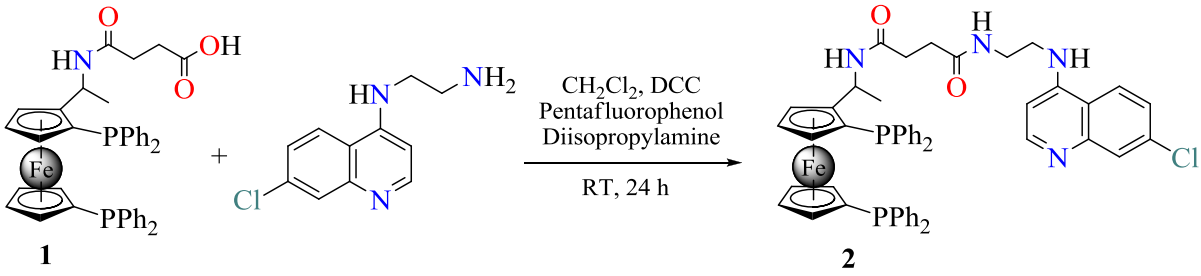

1 **2**

Scheme 1 Synthetic scheme for 1,1'-bis(diphenylphosphino)ferrocene-quinoline conjugate (**2**)

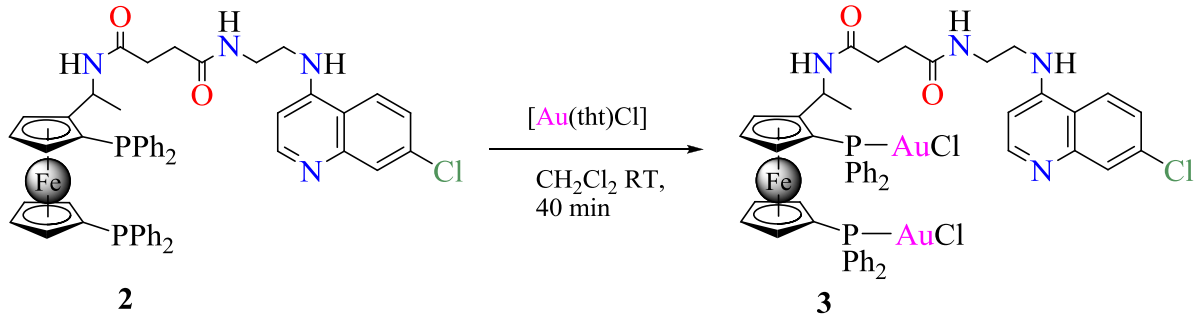

2 **3**

Scheme 2 Synthetic scheme for digold(I) complex **3**

The ^{31}P NMR spectrum of compound **2** shows two phosphorus peaks at -18.00 (s) and -25.69 (s). However, these peaks are considerably downfield shifted upon complexation with gold and appeared at 27.29 (s) and 22.18 (s) (**Fig. S4**). The molecular structure of complex **3**

was determined by X-ray crystallography. Although, the crystal data for **3** did not refine well due to poor crystal quality, the structure is reported primarily for its molecular structure. The molecular structure of complex **3** (**Fig.1**) showed diphenyl phosphine moieties are *trans* to each other because of bulkiness of the groups, with the Au1-P1-P2-Au2 torsion angle ~175°. The geometry around gold is virtually linear and coordination sites are occupied by phosphorus and chloride atoms with P-Au-Cl bond ~175° which is normally observed for bi-coordinated gold(I) complexes (Zhang et al. 2003; Williams et al. 2007; Fonteh et al. 2015).

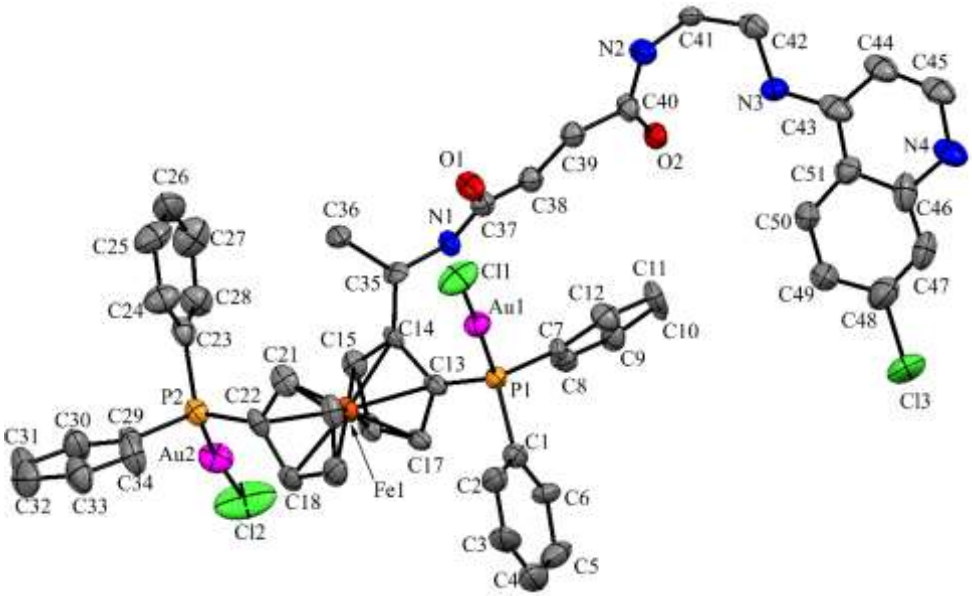

Fig.1 Molecular structure of complex **3** (50% probability ellipsoids). Hydrogen atoms have been omitted for clarity. Selected bond lengths (Å) and angles (°): Au1-P1 = 2.228(3); Au1-Cl1 = 2.280(3); Au2-P2 = 2.222(3); Au2-Cl2 = 2.278(4); P1-C13 = 1.792(11); P2-C22 = 1.787(11); P1-Au1-Cl1 = 174.67(12); P2-Au2-Cl2 = 174.32(18)

Biological Activity

In whole virus assays, **3** displayed remarkable inhibition of the infection of host cells in a dose dependant manner **(Fig.2)**, and the highest concentrations of the complex resulted in percentages of virus inhibition similar to that of the positive control, Nevirapine. TZM-bl cells possess the firefly luciferase reporter gene (LUC), the expression of which is dependent on the presence of the HIV-1 long terminal repeat (LTR) which would be present in infected cells. The addition of the luciferase substrate then results in luminescence (Montefiori 2005). Statistical analysis revealed significantly ($p < 0.05$) decreased luminescence in cells treated with virus pre-incubated with **3** than cells treated with virus only, indicating non-infection. The infection of cells by HIV-1 mainly involves three steps which are (i) the attachment of the viral gp120 protein with the CD-4 T cell receptor, (ii) binding of the gp120 protein with the chemokine receptors CCR5 or CXCR4 and lastly (iii) the fusion of the cell and viral

membranes (Briz et al. 2006). To date, there are only two compounds that have been approved for entry inhibition and these are maraviroc which is a CCR5 inhibitor and enfurvirtide which is a fusion inhibitor (Desai et al. 2012). There is scope for complex **3** to be developed into a member of this class of antiretroviral drugs. As stated before, chloroquine on its own has been reported to inhibit HIV-1 infectivity, however, this was at very high concentrations (96 and 32 µg/mL) (Tsai et al. 1990; Boelaert et al. 1999), indicating improved activity by **3**.

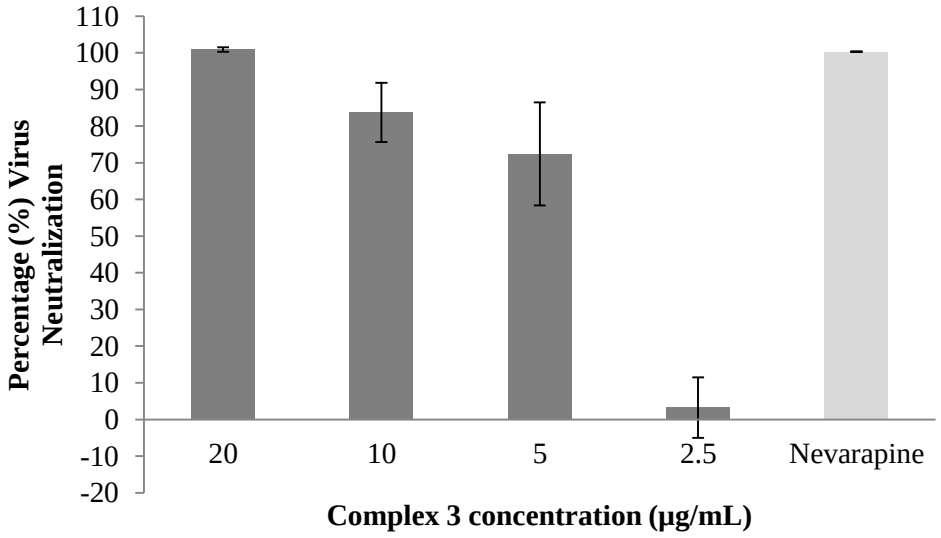

Fig.2 The inhibition of the infection of TZM-bl cells by a pseudovirus, ZM53 in the presence of **3**. The complex caused > 70% neutralisation of pseudovrius at 3 of the 4 tested concentrations. n=3, error bars represent standard error of the mean (SEM)

Effective concentrations of **3** were showed to be non-toxic to the cells, therefore virus inhibition was not due to compound mediated toxicity .The complex resulted in minimal toxicity towards TZM-bl cells; a viability profile exhibiting a dose response is shown in **Fig.3**. Real-time cell electronic sensing confirmed the non-cytotoxicity of complex **3** and all tested concentrations were non-toxic (**Fig.4**). In fact, cells treated with the complex seemed to remain attached to the wells while untreated cells had started to detach and die (Pink curve). The anti-proliferative behaviour of **3** along with the lack of toxicity is indicative of its cytostatic behaviour.

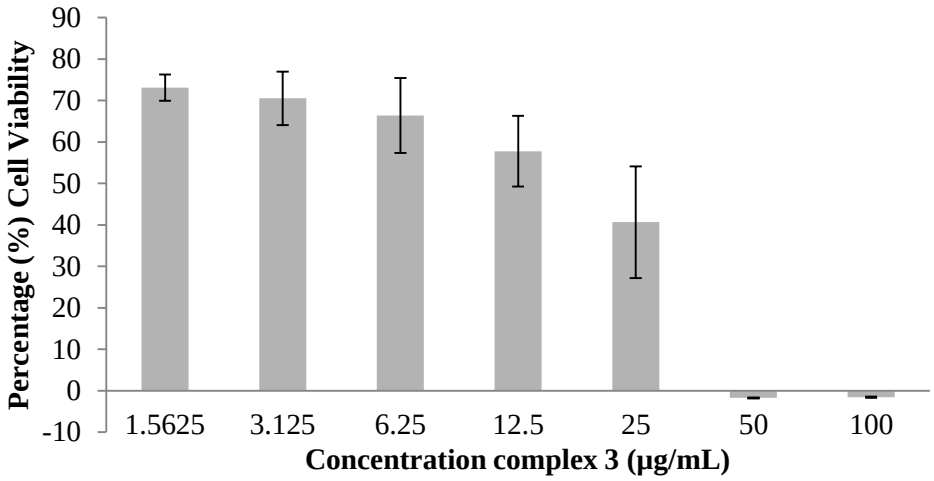

Fig.3 MTT cytotoxicity profile of complex **3** in TZM-bl cells. The predicted CC_{50} of this compound in these cells was 24.34 ± 0.68 µg/mL. n=3, error bars represent standard error of the mean (SEM)

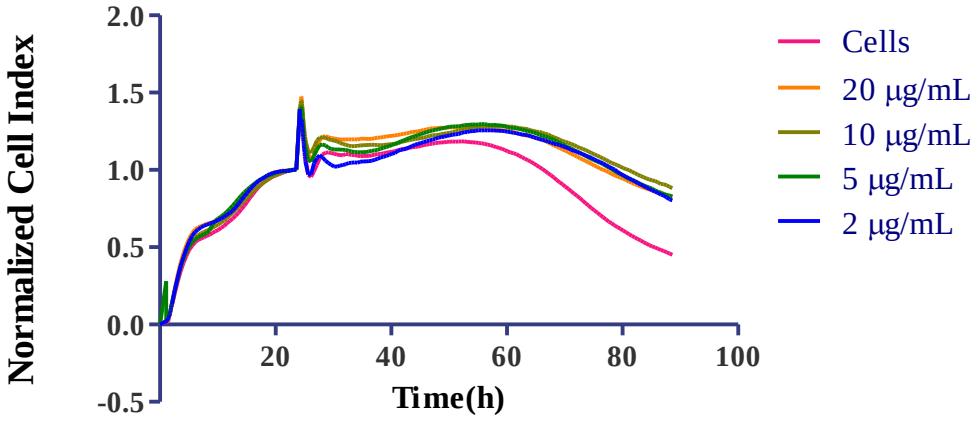

Fig.4 RTCES analysis of compound **3** on TZM-bl cells. All tested concentrations resulted in profiles similar to untreated cells indicating non-toxicity .See **Supplementary Information** for additional data sets

Cell cycle investigations into the effect of 10 µg/mL of the complex on TZM-bl cells, showed a significant decrease in number of cells in the G_0/G_1 phase and increases in the S and the G_2M phases (**Fig.5**), confirming cytostasis. Cytostatic activity has been shown to be largely characterised by G_2/M cell cycle arrest with compounds like resveratrol shown to cause in G_2/M phase accumulation in cells (Schneider et al. 2000). Some cytostatic complexes such as the chemotherapeutic plant isolate epigenin on the other hand exhibited reversible G_2/M cell arrest which is reportedly through the inhibition of $p34^{cdc2}$ kinase activity (Wang et al. 2000).

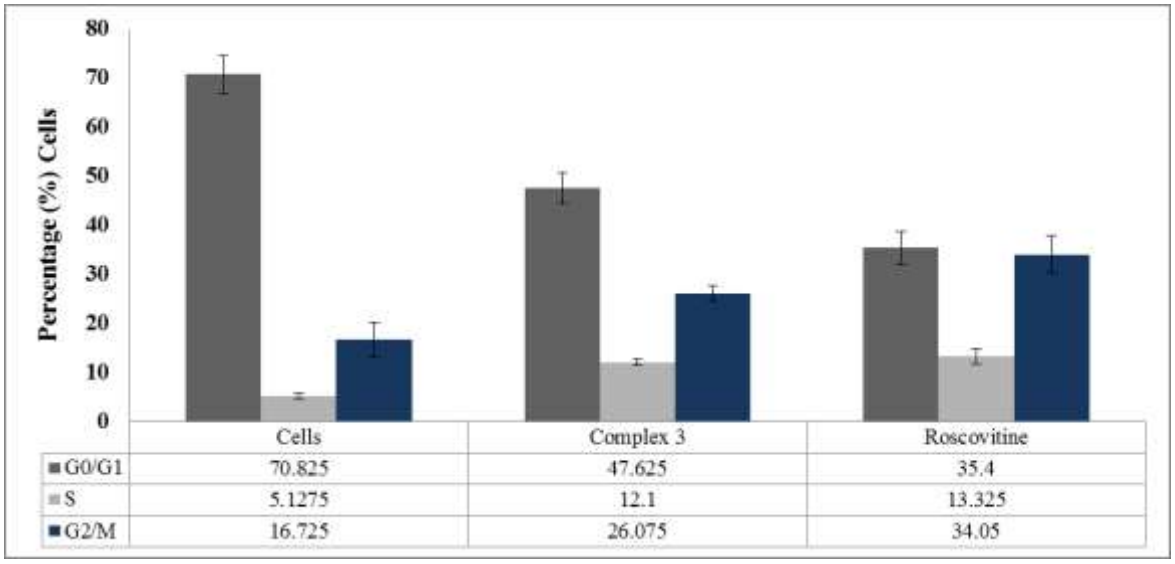

Fig. 5 Effects of complex **3** on the cell cycle of TZM-bl cells. Treatments with **3** (10 µg/mL) resulted in decreased G0/G1 accumulation and increased transition into S and G2/M phases of the cell cycle, similar to the effect of Roscovitine. n=3, error bars represent standard error of the mean (SEM), *$P<0.01$, **$P<0.001$ compared to untreated cells

Complex **3** exhibited a similar cell cycle profile to the cytostatic control roscovitine, which has been shown to inhibit some cyclin-dependent kinases such as erk1 &2, cyclin A and cyclin B that play a role in the intracellular control of cell division (Meijer et al. 1997). It is therefore possible that **3** also exhibit its effects through interaction with these kinases (which is subject to on-going investigations).

In conclusion, a newly synthesised digold chloroquine derivative with significant whole virus inhibition at non-toxic concentrations, which also demonstrated cytostatic activity with significant S and G2/M phase cell arrest, is reported here. This is the first report of such activity for gold derivatives of chloroquine. This combination of antiviral and cytostatic behaviour could remove the necessity of combination drugs, negating negative effects such as drug-drug interactions. This makes **3** a contender for use in HIV-1 infection as a virostatic agent.

Acknowledgements

We would like to thank the National Research Foundation (NRF) and the Technology Innovation Agency (TIA), South Africa for funding the project as well as the NRF Innovation Doctoral Scholarship for N. Gama. K. Kumar would like to thank the European Commission (Erasmus Mundus Europe Asia, EMEA) and University of Johannesburg, South Africa for a postdoctoral fellowship

Electronic supplementary information (ESI) available.

Electronic supplementary information including the following is available: synthetic procedure and characterization for compounds **2** and **3,** ^{1}H, $^{13}C\{^{1}H\}$ and ^{31}P NMR spectra for compounds **2** and **3**, details of crystal data collection and structure refinement parameters, and crystallographic data for structural analysis (in CIF format). CCDC number 1432416.

References

Abid Masood M, Farrant E, Morao I, et al (2012) Lead diversification. Application to existing drug molecules: Mifepristone 1 and antalarmin 8. Bioorganic Med Chem Lett 22:723–728. doi: 10.1016/j.bmcl.2011.10.066

Atienzar F a, Tilmant K, Gerets HH, et al (2011) The use of real-time cell analyzer technology in drug discovery: defining optimal cell culture conditions and assay reproducibility with different adherent cellular models. J Biomol Screen 16:575–87. doi: 10.1177/1087057111402825

Bjelosevic H, Spégel C, Snygg ÅS, et al (2006) Synthesis and structural characterisation of novel platinum-based drug candidates with extended functionality by incorporation of bis(diphenylphosphino)ferrocene units as metal chelators. Tetrahedron 62:4519–4527. doi: 10.1016/j.tet.2006.02.057

Boelaert JR, Sperber K, Piette J (1999) Chloroquine exerts an additive in vitro anti-HIV type 1 effect when associated with didanosine and hydroxyurea. AIDS Res Hum Retroviruses 15:1241–7. doi: 10.1089/088922299310133

Brenchley JM, Schacker TW, Ruff LE, et al (2004) CD4+ T cell depletion during all stages of HIV disease occurs predominantly in the gastrointestinal tract. J Exp Med 200:749–59. doi: 10.1084/jem.20040874

Briz V, Poveda E, Soriano V (2006) HIV entry inhibitors: mechanisms of action and resistance pathways. J Antimicrob Chemother 57:619–27. doi: 10.1093/jac/dkl027

d'Ettorre G, Paiardini M, Ceccarelli G, et al (2011) HIV-associated immune activation: from bench to bedside. AIDS Res Hum Retroviruses 27:355–364. doi: 10.1089/aid.2010.0342

Derdeyn CA, Decker JM, Sfakianos JN, et al (2000) Sensitivity of human immunodeficiency virus type 1 to the fusion inhibitor T-20 is modulated by coreceptor specificity defined by the V3 loop of gp120. J Virol 74:8358–8367.

Desai M, Iyer G, Dikshit RK (2012) Antiretroviral drugs: critical issues and recent advances. Indian J Pharmacol 44:288–98. doi: 10.4103/0253-7613.96296

Fonteh P, Elkhadir A, Omindi B, et al (2015) Impedance technology reveals correlations between cytotoxicity and lipophilicity of mono and bimetallic phosphine complexes. BioMetals. doi: 10.1007/s10534-015-9851-y

Fonteh PN, Keter FK, Meyer D (2011) New bis(thiosemicarbazonate) gold(III) complexes inhibit HIV replication at cytostatic concentrations: potential for incorporation into virostatic cocktails. J Inorg Biochem 105:1173–80. doi: 10.1016/j.jinorgbio.2011.05.011

García F, Plana M, Arnedo M, et al (2003) A cytostatic drug improves control of HIV-1 replication during structured treatment interruptions: a randomized study. AIDS 17:43–51. doi:

10.1097/01.aids.0000042953.95433.79

Krogstad DJ, Gluzman IY, Kyle DE, et al (1987) Efflux of chloroquine from Plasmodium falciparum: mechanism of chloroquine resistance. Science 238:1283–5.

Kustermann S, Boess F, Buness A, et al (2013) A label-free, impedance-based real time assay to identify drug-induced toxicities and differentiate cytostatic from cytotoxic effects. Toxicol Vitr 27:1589–95. doi: 10.1016/j.tiv.2012.08.019

Lori F, Foli A, Groff A, et al (2005) Optimal suppression of HIV replication by low-dose hydroxyurea through the combination of antiviral and cytostatic ("virostatic") mechanisms. AIDS 19:1173–1181.

Lori F, Jessen H, Lieberman J, et al (1999) Immune Restoration by Combination of a Cytostatic (Didanosine and Indinavir). AIDS Res Hum Retroviruses 15:619–624.

Meijer L, Borgne A, Mulner O, et al (1997) Biochemical and Cellular Effects of Roscovitine, a Potent and Selective Inhibitor of the Cyclin-Dependent Kinases cdc2, cdk2 and cdk5. Eur J Biochem 243:527–536. doi: 10.1111/j.1432-1033.1997.t01-2-00527.x

Montefiori DC (2005) Evaluating neutralizing antibodies against HIV, SIV, and SHIV in luciferase reporter gene assays. Curr Protoc Immunol Ed by John E Coligan al Chapter 12:Unit 12.11.

Montessori V, Press N, Harris M, et al (2004) Adverse effects of antiretroviral therapy for HIV infection. CMAJ 170:229–238.

Mufhandu HT, Gray ES, Madiga MC, et al (2012) UCLA1, a synthetic derivative of a gp120 RNA aptamer, inhibits entry of human immunodeficiency virus type 1 subtype C. J Virol 86:4989–99. doi: 10.1128/JVI.06893-11

Muthyala R (2011) Orphan/rare drug discovery through drug repositioning. Drug Discov Today Ther Strateg 8:71–76. doi: 10.1016/j.ddstr.2011.10.003

Palatinus L, Chapuis G (2007) SUPERFLIP - a computer program for the solution of crystal structures by charge flipping in arbitrary dimensions. J Appl Crystallogr 40:786–790.

Platt EJ, Bilska M, Kozak SL, et al (2009) Evidence that ecotropic murine leukemia virus contamination in TZM-bl cells does not affect the outcome of neutralizing antibody assays with human immunodeficiency virus type 1. J Virol 83:8289–92.

Platt EJ, Wehrly K, Kuhmann SE, et al (1998) Effects of CCR5 and CD4 cell surface concentrations on infections by macrophagetropic isolates of human immunodeficiency virus type 1. J Virol 72:2855–2864.

Pollack TM, Mccoy C, Pharm D, Stead W (2009) Clinically Significant Adverse Events from a Drug Interaction Between Quetiapine and Atazanavir-Ritonavir in Two Patients. Pharmacotherapy 29:1386–1391.

Sánchez-Delgado R a, Anzellotti A (2004) Metal complexes as chemotherapeutic agents against tropical diseases: trypanosomiasis, malaria and leishmaniasis. Mini Rev Med Chem 4:23–30.

Savarino A, Gennero L, Sperber K, Boelaert JR (2001) The anti-HIV-1 activity of chloroquine. J Clin Virol 20:131–5.

Schneider Y, Vincent F, Duranton B, et al (2000) Anti-proliferative effect of resveratrol, a natural component of grapes and wine, on human colonic cancer cells. Cancer Lett 158:85–91. doi: 10.1016/S0304-3835(00)00511-5

Sheldrick GM (2008) A short history of SHELX. Acta Crystallogr 64:112–122.

Spek AL (2009) Structure validation in chemical crystallography. Acta Crystallogr D65:148–155.

Takeuchi Y, McClure MO, Pizzato M (2008) Identification of γ-retroviruses constitutively released from cell lines used for HIV research. J Virol 82:12585–8.

Tsai WP, Nara PL, Kung HF, Oroszlan S (1990) Inhibition of human immunodeficiency virus infectivity by chloroquine. AIDS Res Hum Retroviruses 6:481–489.

Uson R, Laguna A, Laguna M, et al (1989) (Tetrahydrothiophene)Gold(I) or Gold(III) Complexes. Inorg Synth 26:85–91.

Wang W, Heideman L, Chung CS, et al (2000) Cell-Cycle Arrest at G2 / M and Growth Inhibition by Apigenin in Human Colon Carcinoma Cell Lines. Mol Carcinog 28:102–110.

Wei X, Decker J, Liu H, et al (2002) Emergence of resistant human immunodeficiency virus type 1 in patients receiving fusion inhibitor (T-20) monotherapy. Antimicrob Agents Chemother 46:1896–1905. doi: 10.1128/AAC.46.6.1896

Williams DBG, Traut T, Kriel FH, van Zyl WE (2007) Bidentate amino- and iminophosphine ligands in mono- and dinuclear gold(I) complexes: Synthesis, structures and AuCl displacement by AuC6F5. Inorg Chem Commun 10:538–542. doi: 10.1016/j.inoche.2007.01.022

World Health Organization (2015) Media centre - HIV / AIDS.

Yearick K, Ekoue-kovi K, Iwaniuk DP, et al (2008) Overcoming Drug Resistance to Heme-Targeted Antimalarials by Systematic Side Chain Variation of 7-Chloro-4-aminoquinolines. J Med Chem 51:1995–1998.

Zhang Q, Hua G, Bhattacharyya P, et al (2003) Syntheses and coordination chemistry of aminomethylphosphine derivatives of adenine. Eur J Inorg Chem 2003:2426–2437. doi: 10.1002/ejic.200300037

Supporting Information

Decision tree by Kusterman et al. (2013)

The following decision tree was used in order to determine if the complex exhibited significant toxicity or not as determined by real-time cell electronic sensing.

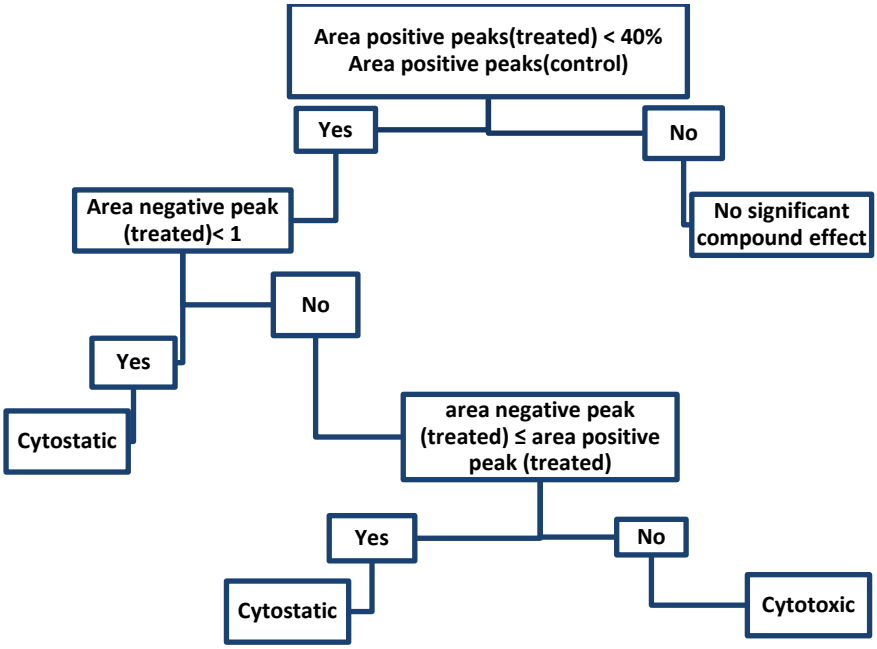

Fig. S1 Decision tree for the determination of cytotoxity in RTCES (Kustermann et al., 2013)

X-ray structure determinations

The crystallographic details of complex **3** are summarized in **Table S1.**

Table S1 Crystal data and structure refinement parameters for complex **3**

	3
empirical formula	$C_{51}H_{47}Au_2Cl_3FeN_4O_2P_2$
Fw	1366.00
temp (K)	170(2)
λ(Å)	0.71073
cryst syst	Triclinic
space group	P $\bar{1}$
a (Å)	9.6495(5)
b (Å)	14.8527(16)
c (Å)	22.1859(8)
α (deg)	88.083(6)
β (deg)	89.310(4)
γ (deg)	77.291(7)
V (Å^3)	3100.0(4)
Z	2
ρ_{calc} (Mg/m^3)	1.463
μ(Mo Kα) (mm^{-1})	5.168
No. reflns.	24634
Unique reflns.	14886
GOOF (F^2)	1.041
R_{int}	0.0447
R1[a] ($I \geq 2\sigma$)	0.0808
wR2[b] ($I \geq 2\sigma$)	0.1894

[a] $R1 = \Sigma||F_o| - |F_c||/\Sigma|F_o|$. [b] $wR2 = [\Sigma[w(F_o^2 - F_c^2)^2]/ \Sigma[w(F_o^2)^2]]^{1/2}$.

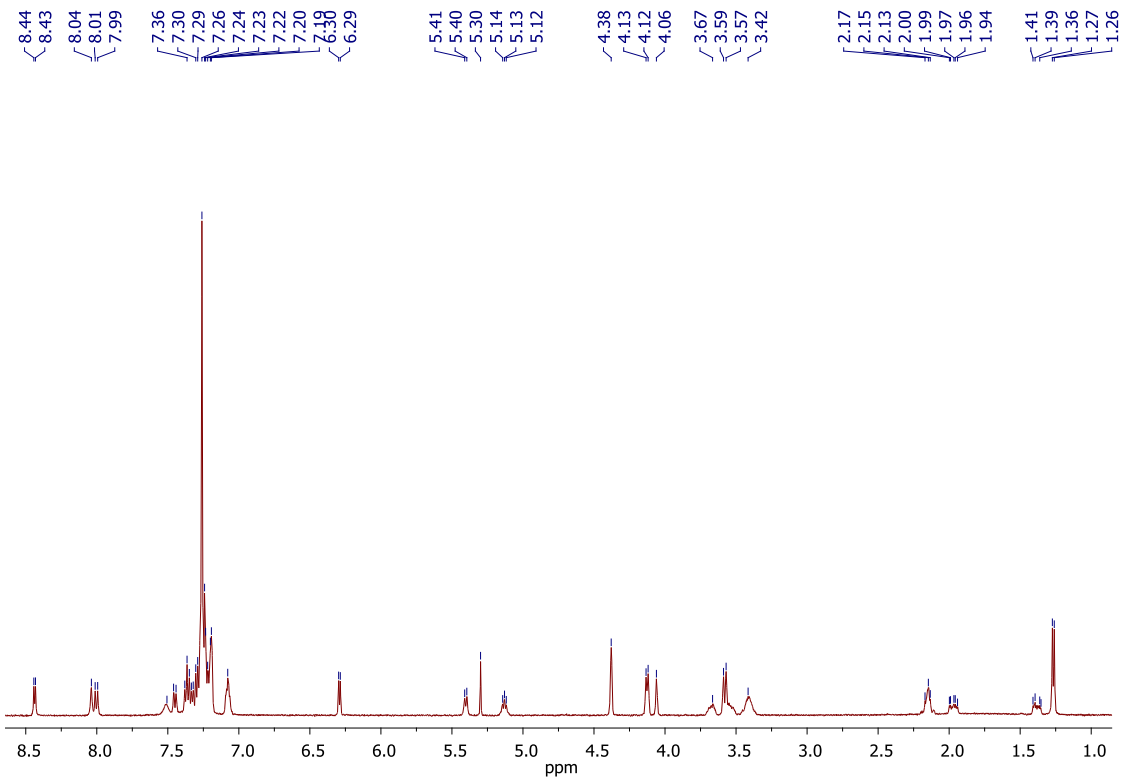

Fig. S2 ^{1}H NMR spectrum for compound **2**

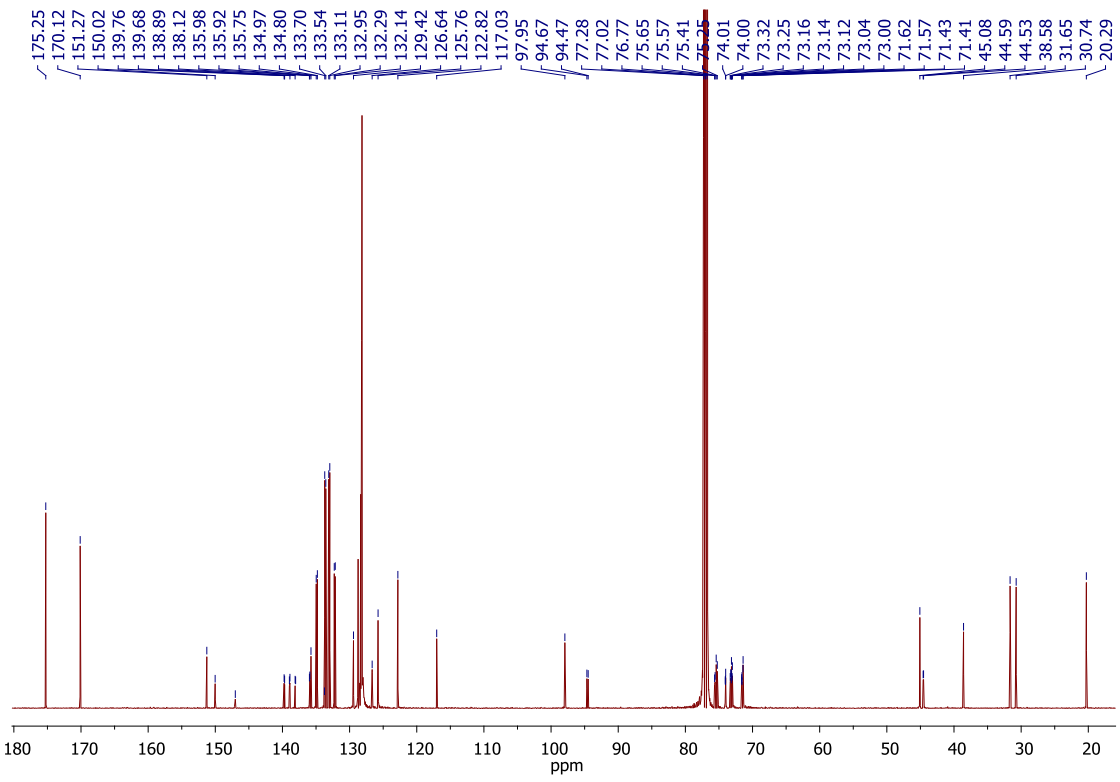

Fig. S3 ^{13}C{^{1}H} NMR spectrum for compound **2**

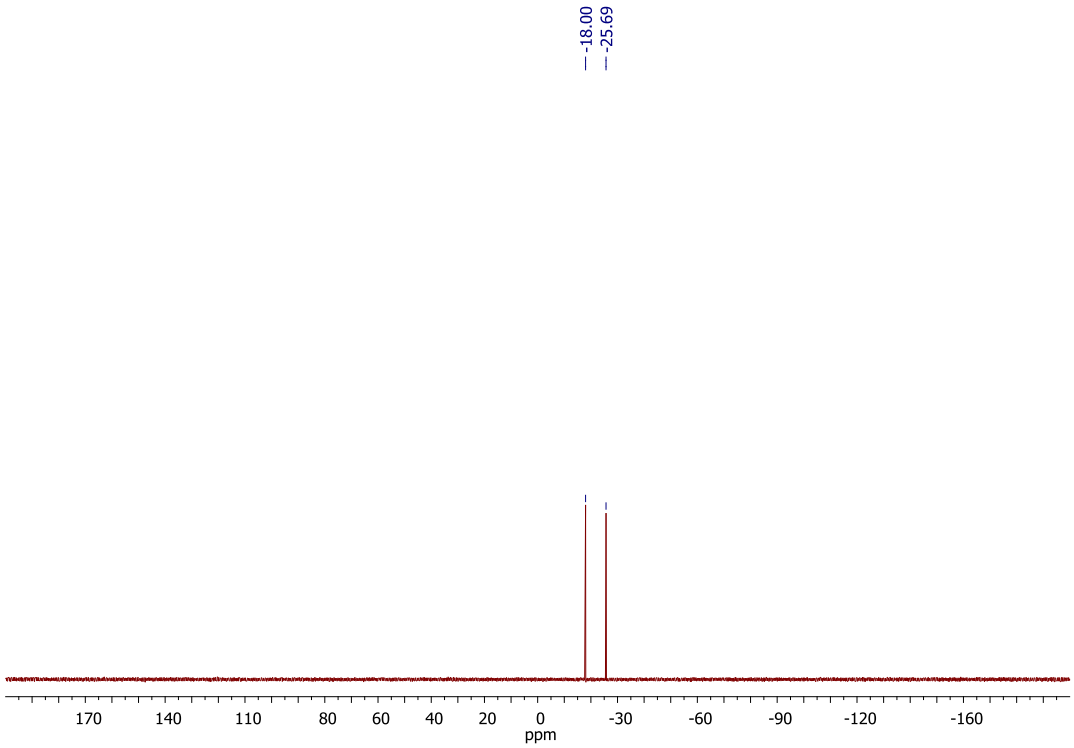

Fig. S4 ^{31}P NMR spectrum for compound **2**

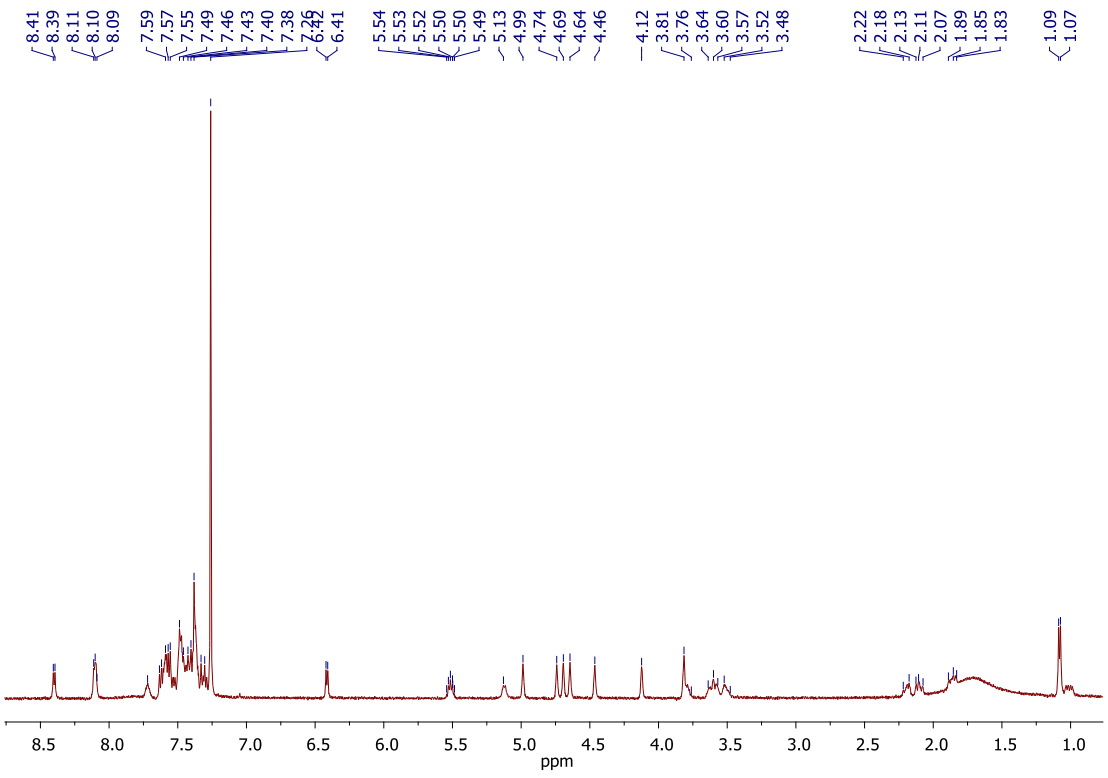

Fig. S5 ^{1}H NMR spectrum for complex **3**

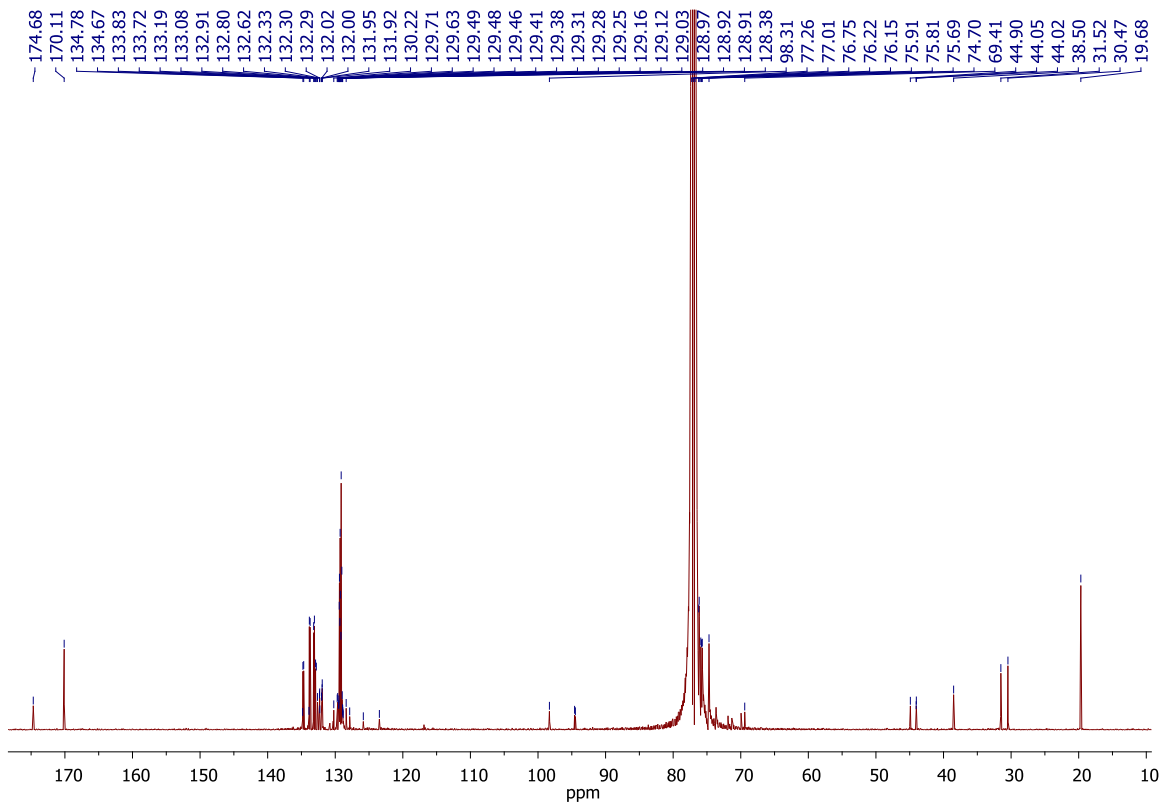

Fig S6 $^{13}C\{^{1}H\}$ NMR spectrum for complex **3**

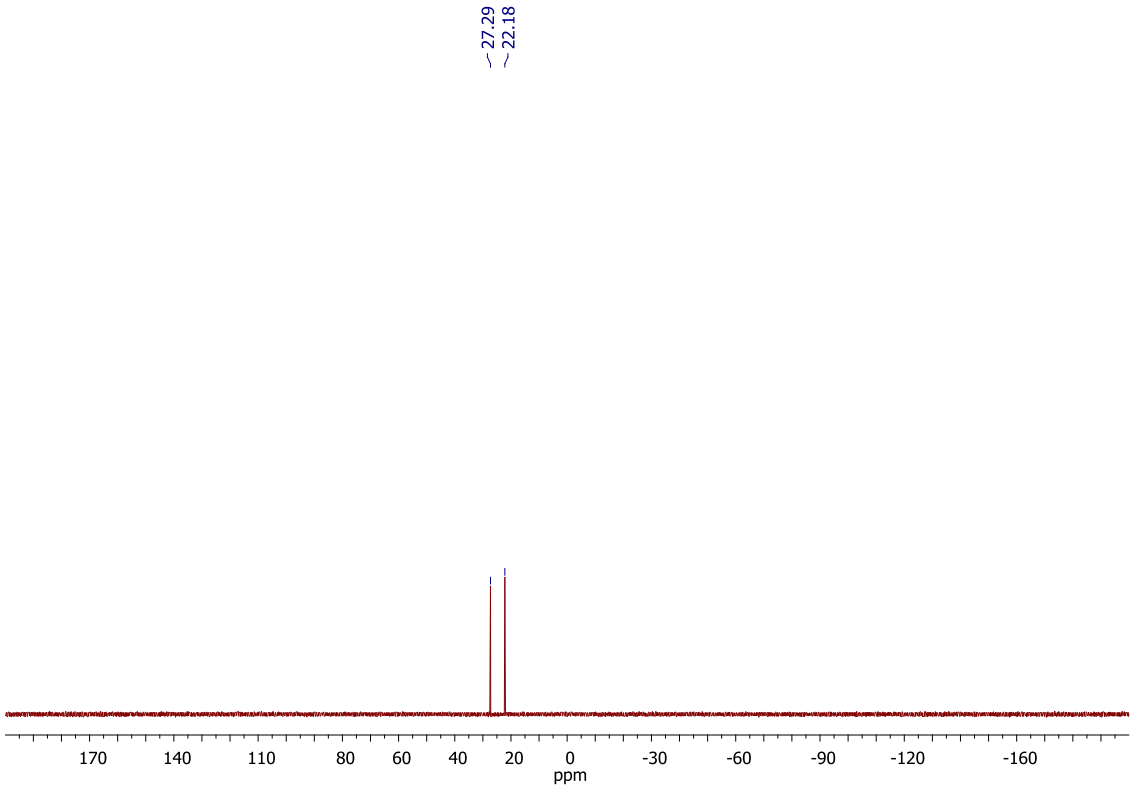

Fig.S7 ^{31}P NMR spectrum for complex **3**

Real-time cell electronic sensing

Three biological repeats were performed in the evaluation of complex **3** on the real-time effects on TZM-bl cells. **Fig.S8** shows two additional data sets of the analysis.

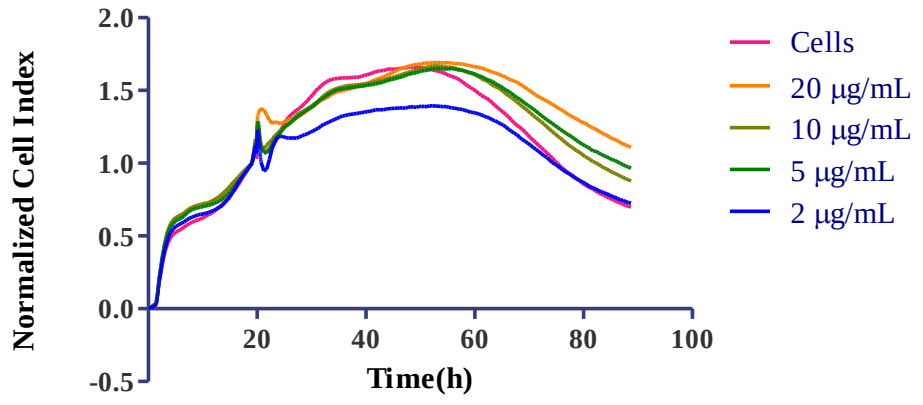

(A)

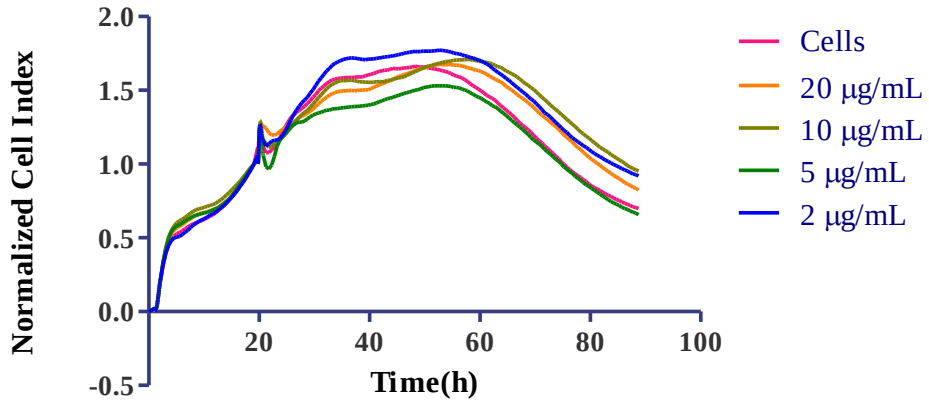

(B)

Fig. S8 Real-time cell electronic sensing analysis of **3**. TZM-bl cells were treated with various concentrations of 3 and growth profiles similar to untreated cells where observed indicating the non-toxicity of this complex at these concentrations.